

Chapter 18

Fractal-Based Analysis of Arteriovenous Malformations (AVMs)

Antonio Di Ieva and Gernot Reishofer

Abstract Arteriovenous malformations (AVMs) are cerebrovascular lesions consisting of a pathologic tangle of the vessels characterized by a core termed the nidus, which is the “nest” where the fistulous connections occur. AVMs can cause headache, stroke, and/or seizures. Their treatment can be challenging requiring surgery, endovascular embolization, and/or radiosurgery as well. AVMs’ morphology varies greatly among patients, and there is still a lack of standardization of angioarchitectural parameters, which can be used as morphometric parameters as well as potential clinical biomarkers (e.g., related to prognosis).

In search of new diagnostic and prognostic neuroimaging biomarkers of AVMs, computational fractal-based models have been proposed for describing and quantifying the angioarchitecture of the nidus. In fact, the fractal dimension (FD) can be used to quantify AVMs’ branching pattern. Higher FD values are related to AVMs characterized by an increased number and tortuosity of the intranidal vessels or to an increasing angioarchitectural complexity as a whole. Moreover, FD has been investigated in relation to the outcome after Gamma Knife radiosurgery, and an inverse relationship between FD and AVM obliteration was found.

Taken altogether, FD is able to quantify in a single and objective value what neuro-radiologists describe in qualitative and/or semiquantitative way, thus confirming FD as a reliable morphometric neuroimaging biomarker of AVMs and as a potential surrogate imaging biomarker. Moreover, computational fractal-based techniques are under investigation for the automatic segmentation and extraction of the edges of the nidus in neuroimaging, which can be relevant for surgery and/or radiosurgery planning.

A. Di Ieva, MD, PhD (✉)

Neurosurgery Unit, Faculty of Medicine and Health Sciences, Macquarie University, Sydney, Australia

Garvan Institute of Medical Research, Sydney, NSW, Australia

Medical University of Vienna, Vienna, Austria

University of Toronto, Toronto, ON, Canada

e-mail: diieva@hotmail.com

G. Reishofer (✉)

Department of Radiology, MR-Physics, Medical University of Graz, Graz, Austria

e-mail: gernot.reishofer@medunigraz.at

Keywords Angioarchitecture • Arteriovenous malformation • AVM • Box counting • Fractal dimension • Gamma Knife radiosurgery • Minkowski dimension • Outcome

18.1 Introduction

Arteriovenous malformations (AVMs) are vascular lesions of the brain and, more rarely, of the spinal cord, occurring with an incidence of 1/100,000/year and prevalence of 18/100,000/year [1]. In about 70% of cases, AVMs present with hemorrhage, accounting for 2% of all strokes, while in 20% of patients, seizures are the first presentation. In some cases, AVMs can be asymptomatic or can cause headache, focal neurological deficits, cognitive dysfunction, and pulsatile tinnitus. The combined rate of mortality and major morbidity related to untreated AVMs is of 2.7% per year [22].

Morphologically, AVMs consist of a pathologic tangle of vessels, i.e., fistulous connections of afferent arteries draining blood directly into dilated efferent draining veins without the interposition of the brain parenchyma (Fig. 18.1). The core of the AVMs is defined as the nidus, which is the nest where the pathologic connections occur. Their treatment can be challenging requiring surgery (by means of microneurosurgery techniques), endovascular embolization or radiosurgery (e.g., Gamma Knife), or a combination of such modalities. The aim of the treatment is the removal and/or obliteration of the nidus in order to lower the risk of bleeding and/or seizures.

Several systems have been proposed to classify AVMs, with the most used and clinically relevant being the Spetzler-Martin classification system [28] and its subsequent modification, the Spetzler-Ponce classification system [27]. Both systems quantify specific features in a final score, i.e., (a) the size of the nidus, (b) the functional eloquence of the brain region where the AVM is located, and (c) the type of venous drainage. On one hand these systems are very relevant because they are related to outcome (prognostication) and therapy modality, but on the other hand no information is added in regard to the angioarchitecture. AVMs with the same score can show completely different shapes, different number of vessels forming the nidus, peculiar branching patterns, and distinct geometrical complexity. To overcome this limitation, several methods have been proposed for the morphometric analysis of AVMs, including a computational fractal-based approach, as discussed in this chapter.

18.2 Neuroimaging of AVMs

The diagnosis of AVMs is based on multimodal imaging techniques, which encompass various magnetic resonance imaging (MRI) techniques, computed tomography (CT), and catheter biplane digital subtraction angiography (DSA), which is still

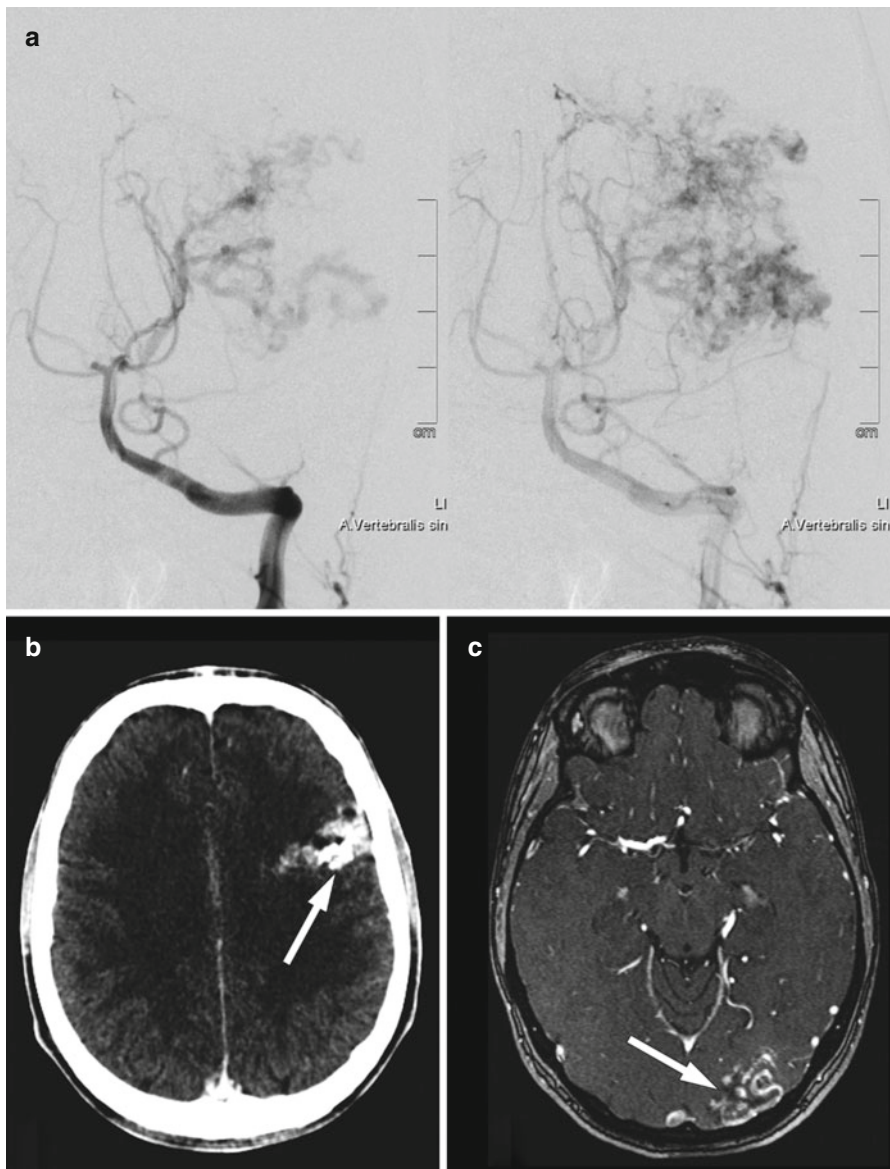


Fig. 18.1 CTA and MRA for different patients with AVM. (a) DSA of the vertebral artery imaged in an earlier phase (*left*) giving more weight to the feeding arteries and imaged in a later phase (*right*) giving a better contrast to the nidus. (b) CTA and (c) MRA of a unilateral AVM of two different patients marked with a *white arrow*

considered as the gold-standard technique [21] (Fig. 18.1). The high temporal resolution of DSA allows the subsequent subtraction of a baseline image from contrast-enhanced images. Different states of contrast media uptake provide an excellent differentiation between the arteries, the veins, and the nidus. However, since this technique only generates 2D information from two orthogonal directions, the entire geometrical complexity of the nidus and the vascular system is not fully represented. Magnetic resonance angiography (MRA) and computed tomography angiography (CTA) overcome this limitation and provide a 3D representation of the vasculature. In MRA, techniques with contrast media (CE-MRA) or without contrast media (TOF-MRA) can be used to visualize the vascular tree. A disadvantage of all standard 3D techniques utilizing contrast media (MRA and CTA) is given by the fact that generated images are snapshots of the contrast media flowing through the vascular system. This means that imaging an early phase put stronger weights on the arterial system while imaging a later phase puts more weights on the venous system. The time between bolus injection and data acquisition is therefore crucial for the image quality and a challenging task. 4D techniques that are available for both MR and CT are able to measure sequential angiograms and allow analyzing the dynamics of the flow within the AVM. Dynamic CT angiography (dCTA) provides good spatial and temporal resolution but expose the patient to a high dose of ionizing radiation [20]. In MRI, dynamic contrast-enhanced sequences (DCE-MRI) based on T1-weighted MR scans are used to provide an overview about the AVM flow dynamics (Fig. 18.2), but this technique is limited in spatial and temporal resolution. Recent developments in MR imaging utilize advanced imaging reconstruction techniques such as highly constrained back projection with phase contrast as a constrained (HYPR flow) to improve spatial and temporal resolution [29].

For the optimal representation of the acquired data, several techniques exist for image fusion in multimodal imaging and 3D rendering of the AVM [29].

18.3 AVMs' Angioarchitecture Morphometrics

AVMs vary greatly among patients, and experts have attempted to classify them based on several angioarchitectural parameters, by looking for similar clinical presentation and posttreatment outcome. However, these parameters have not been standardized.

An objective morphostructural analysis of AVMs should provide useful information for classification, prognostication, therapeutic decisions and follow-up.

Several grading systems have been proposed, which generally take into account the number of feeding arteries from the different vascular territories, the size and location of the AVM, and other features, with the Spetzler-Martin (5-tiered score) and Spetzler-Ponce (3-tiered score) as the most clinically relevant and used ones, as previously quoted. By the way, such classification systems do not take into account the morphological complexity of the nidus, referring to its geometry only in terms of the size. Of course, AVMs having the same Euclidean parameters (i.e., maximal

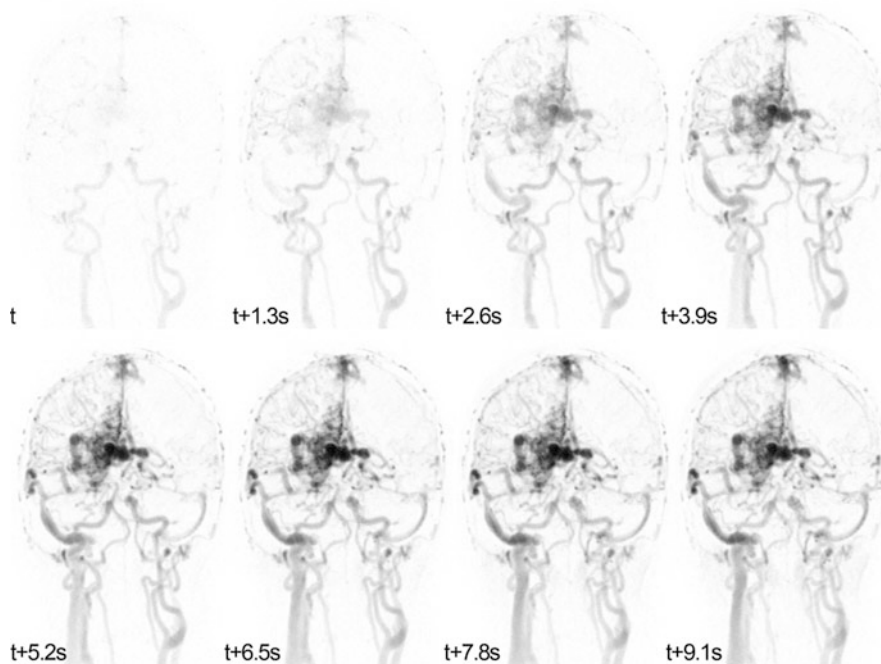


Fig. 18.2 Maximum intensity projection of a 4D dynamic MRA with a temporal resolution of 1.3 s (Images are displayed in inverted view)

diameter and volume) may have a very different pattern of distribution of the vessels forming the nidus (e.g., different density, compactness, tortuosity of the vessels, in one word, different angioarchitecture). Moreover, the distribution of the vessels within the nidus can leave different grades of “gaps” among the vessels themselves. According to the nonlinearity of the AVM’s shape, “compactness” and “diffuseness” of the nidus have been investigated as a better mean of quantification; these parameters have been shown to be important factors in predicting the difficulty to resect an AVM [11].

Fractal analysis is a novel computer-aided mathematical model, which has also been shown to have several applications in clinical neurosciences, including neuroimaging [7]. Fractal dimension and lacunarity seem to offer valid tools to quantify AVM’s geometrical complexity, as presented hereinafter.

18.4 Computational Fractal-Based Analyses of AVMs

Fractal analysis is a mathematical model that, among other parameters, offers the fractal dimension (FD) and lacunarity as measures of the roughness and/or geometrical complexity of natural objects, including physiological and pathological brain

structures in neuroimaging. As several natural objects characterized by a branching pattern, AVMs are suitable to fractal analysis as well. Computing FD of the nidus by means of the box-counting method, for example, adds an objective morphometric parameter to quantify the space-filling properties of the tangle itself, thus offering a potential morphometric biomarker, which could be added into the existing classification systems.

18.4.1 AVMs' Fractal Dimension

The first study that investigated AVMs by means of FD was published by Reishofer et al. in 2012 [25]. Given the fact that the direct observation of the nidus' vasculature using MRI angiography is not an easy task due to limited spatial resolution, the architecture of surrounding arteries was analyzed by means of different measures of FD. The nidus can be supplied by one or more feeding arteries that are directly connected to draining veins leading to a vascular system with a higher geometrical complexity compared to a normal vascular system. The aim of this study was to investigate whether FD, obtained from 3D-time-of-flight (TOF) MR images, is a suitable biomarker to represent changes in the vascular geometry and furthermore whether FD is related to pathologic and physiological parameters such as the nidus size and vascular flow.

Ten patients with a unilateral supratentorial AVM and ten healthy controls participated in this study. The patients and controls underwent a standard MR imaging protocol including T_1 - and T_2 -weighted sequences, 3D-TOF, and dynamic contrast-enhanced (DCE) MR imaging. 3D-TOF MR angiography is an imaging technique that allows the visualization of the cerebral arterial system with high accuracy up to small vessel diameters. The following parameters were used to visualize cerebral arteries covering the circle of Willis and vertebral-basilar arteries: TR = 22 ms, TE = 3.68 ms, flip angle = 18° , FOV = 200 mm, phase FOV = 75%, image matrix = 384×288 , number of slabs = 3, slices/slab = 52, and slice thickness = 0.65 mm. DCE-MRI data were acquired to image the vascular flow using a 3D-FLASH sequence with the following parameters: TR = 2.67 ms, TE = 1.05 ms, flip angle = 16° , FOV = 230 mm, image matrix = 320×320 , number of slabs = 1, slices/slab = 12, and slice thickness = 6 mm. A dose of 0.2 ml/kg body weight contrast agent (ProHance®, Bracco Diagnostics, Inc., Princeton, NJ, USA) was injected intravenously via a power injector (Spectris; Medrad Inc., Indianola, PA, USA) at a flow rate of 3 ml/s. All measurements were carried out on a 3 T Tim Trio system (Siemens Medical Systems, Erlangen, Germany) using a 12-channel head coil. The following image processing steps have been applied in order to prepare 3D-TOF data for fractal analysis (Fig. 18.3):

- Normalization to the standard MNI space (Montreal Neurological Institute) by means of linear co-registration using FLIRT [16] from the FMRIB Software Library (FMRIB Centre, University of Oxford, UK; <http://www.fmrib.ox.ac.uk/>)

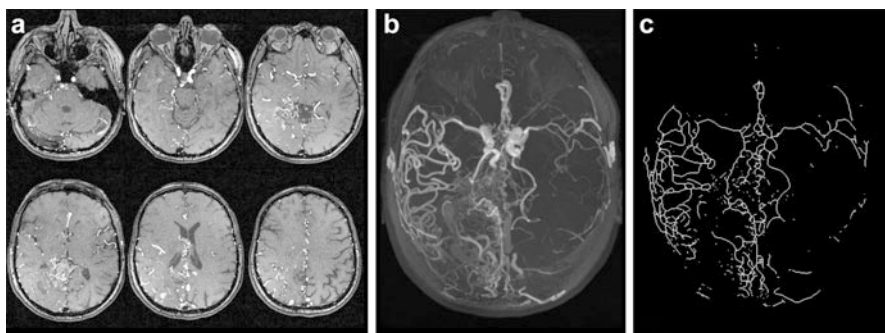


Fig. 18.3 Normalized 3D-TOF images (a) provide the basis for MIP images (b). FD evaluated from MIP images after the image processing step segmentation, binarization, and skeletonization (c) (From Reishofer et al. [25])

fsl/fsl/downloading.html) to account for intersubject variability regarding head size and FOV positioning.

- Maximum intensity projection (MIP) was performed to generate a two-dimensional representation of the 3D-TOF data using MRICro software (Chris Rorden, University of Nottingham, UK; <http://www.nitrc.org/frs/download.php/414/mrzip.zip>).
- The background was separated from the vascular tree using a k-means clustering algorithm.
- Images were converted into binary images and skeletonized using the ImageJ software v.1.45 (Wayne Rasband, National Institutes of Health, USA; <http://rsbweb.nih.gov/ij/download.html>).
- To enable a statistical comparison between the hemisphere with AVM and the hemisphere without AVM for both, patients and controls, the images (364× pixel) were split into two halves (182×436 pixel) and analyzed separately.

The fractal dimension was approximated using the box-counting dimension (D_b) and the Minkowski dimension (D_m) [17]. All of the fractal measurements were evaluated for the whole brain in patients (P_{total}) and healthy controls (HC_{total}) and also for both hemispheres separately in patients (P_{AVM} , $P_{no\ AVM}$) and controls (HC_{left} , HC_{right}). A 2×2 mixed-design ANOVA test with a within-subject factor of hemisphere (for patients, AVM, no AVM; for healthy controls, left, right) and a between-subject factor of group (P, HC) was applied to test for significant differences.

Patients showed significantly higher FD values for both methods in hemispheres with AVM compared with the hemispheres without AVM (D_b , $p=0.002$; D_m , $p=0.002$). Controls had similar values for FD in both hemispheres with no significant differences in FD (D_b , $p=0.982$; D_m , $p=0.892$). No significant differences were observed comparing the non-affected hemisphere of patients with healthy controls (HC_{left} , D_b , $p=0.574$; D_m , $p=0.918$; HC_{right} , D_b , $p=0.691$; D_m , $p=0.872$) but significant differences when comparing the patient's hemisphere with AVM with the hemispheres of healthy controls (HC_{left} , D_b , $p=0.015$; D_m , $p=0.020$; HC_{right} , D_b , $p=0.010$; D_m , $p=0.024$) (Fig. 18.4).

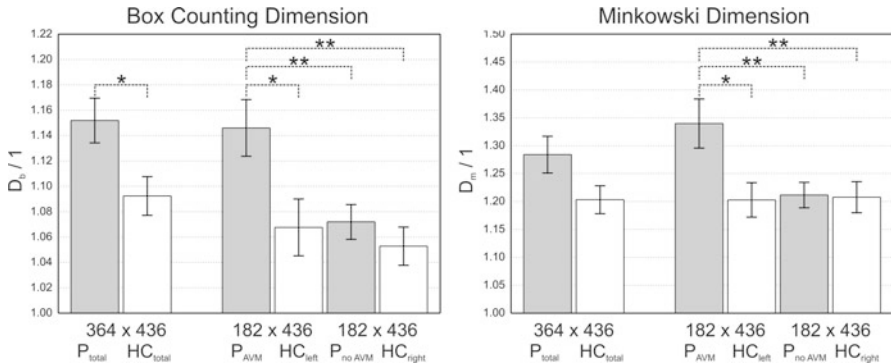


Fig. 18.4 Mean values of D_b (left side) and D_m (right side) comparing patients (P_{total}) with healthy controls (HC_{total}) for the whole image, hemispheres of patients with AVM (P_{AVM}) compared to the hemisphere without AVM ($P_{no\ AVM}$), and comparison of the left and right hemispheres of healthy controls (HC_{left} , HC_{right}). Asterisks indicate significant differences in group comparisons: * $p < 0.05$, ** $p < 0.01$

These results suggest that FD is a sensitive parameter able to detect changes in the geometrical complexity of the cerebral arterial system with high accuracy.

Values of FD are strongly correlated to physiological and pathologic parameters. This has been demonstrated by correlating FD with the maximum slope of contrast media transit obtained from dynamic contrast-enhanced (DCE) MRI data. A linear regression analysis showed a strong and positive linear correlation between FD of the affected hemisphere and the maximum slope of contrast media transit for D_b and D_m (D_b , $r = 0.913$; $p < 0.0001$; D_m , $r = 0.926$; $p < 0.0001$) (Fig. 18.5). Given the fact that the amount of arterial inflow is related to the number of vessels feeding the nidus, this result was not unexpected. A strong correlation was also found between FD and the nidus size (D_b , $r = 0.944$; $p < 0.0001$; D_m , $r = 0.963$; $p < 0.0001$). The nidus size was estimated from DSA data. This strong correlation is not that obvious but suggests that there is a relation between vascular complexity and nidus size.

It has to be noted that absolute values obtained from the box-counting method are dependent from the image matrix size [24]. Giving the fact that the box size is doubled at each iteration step starting with the size of 1 pixel, a complete covering of the image is only possible if the dimensions of the image to be analyzed are given as a power of two. If this is not the case, FD is dependent from the initial location of the grid. To overcome these limitations in the box-counting method, extensions of this technique have been proposed [19] such as the sliding box-counting dimension. When using this technique, each box is slid over the image overlapping the previous box making this method independent from the initial state but at the cost of computational time. The assessment of FD by evaluating the Minkowski dimension uses a different concept in which the structure itself is covered through geometrical objects such as circles, triangles, or squares making this method independent from different image matrix sizes. Another limitation is given by the fact that an MIP of 3D-TOF MR images is only an approximate representation of the vascular system. Superimposed

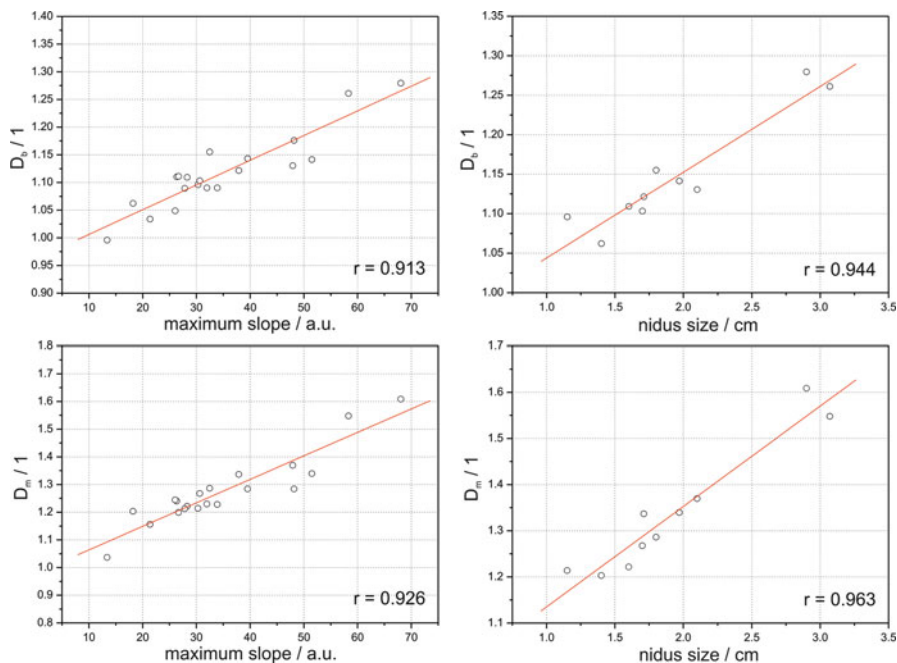


Fig. 18.5 Correlation between FD values (D_b , D_m) and the maximum slope of contrast media transit obtained from DCE-MRI data (*first column*) and correlation between FD values (D_b , D_m) and the nidus size evaluated from X-ray angiography data (*second column*)

vessels cannot be discriminated for a fixed projection plane, but since the projection of a fractal from an m -dimensional space into a $(m-1)$ dimensional subspace is well defined [12], FD from MIP images is an acceptable approximation. However, FD analysis of the vascular cerebral system is a simple and robust technique that yields an objective measure and may assist neuroradiologists in the diagnosis of complex cerebrovascular diseases.

18.4.2 Fractal Dimension of the Nidus and Its Relevance in Radiosurgery

Di Ieva et al. investigated the applicability of FD as a potential neuroimaging biomarker of the AVMs' angioarchitecture, especially in relation to the patients' outcome and follow-up in radiosurgery [9]. The Gamma Knife (GK) radiosurgery treatment, as well as other radiosurgical modalities, is aimed to obliterate the fistulous connections within the nidus, lowering the risk of bleeding. By means of specialized equipment, the stereotactic GK focuses multiple beams of radiation on the target (e.g., a brain tumor or AVM). The radiosurgical effect of obliteration of the vessels occurs over time, in general in 2–3 years; the 3-year obliteration rates following stereotactic

radiosurgery range from 60 to 86.6% [3, 13, 23]. The box-counting method was used for the FD computation in a retrospective case series of 54 patients affected by brain AVMs who underwent GK radiosurgery at the University of Toronto (Ontario, Canada) [9]. In this study, almost 54% of patients presented with hemorrhage, 13% only with headache, 9% with seizures, while other patients were incidentally diagnosed or reported minor focal neurological deficits. All of the patients underwent multimodal imaging, including CTA, MRA, and angiogram as well, but in order to standardize the image and the following fractal analysis, only MRA images performed on the same scanner with the same parameters were considered in the analysis. By means of such selection in the inputs (see the “black box” concept in Chap. 12), it was possible to obtain a homogeneous dataset for analysis. 3T GE Medical System Signa HDxt with an eight-channel head coil was used for all patients, with the following MRI parameters: axial 2D FRSE sequence with a rectangular matrix of 320, echo train length of 15, TR of 5,500 ms and TE of 91 ms, slice thickness of 2 mm without interslice gap, and with a rectangular field of view of 20 cm resulting in plane resolution of 0.625 mm square. Images were transferred to the radiosurgery software, which is a modification of CMI software (Montreal Stereotactic Planning System; CMI Services, Montreal, QC, Canada) [2] (see methods in [9]). A 4C GK radiosurgery system (Leksell Gamma Knife® Perfexion™, Sweden) was used for the stereotactic radiosurgery treatment. A standard dose of 25 Gray (Gy) for AVM volumes <4 cm³ and 20 Gy for volumes >4 cm³ was administered (limiting to 15 Gy the dose to the nidus whether near to eloquent brain areas). Checking the imaging 3 years after the treatment, the outcome of radiosurgery was dichotomized as complete obliteration, defined as the total disappearance of the nidus on the MRA, no abnormal flow voids on MRI and no early draining vein on the angiogram.

The image analysis was based on the following steps (Fig. 18.6):

- Selection of the MR sequences (FRFSE T2 post-gadolinium) and images containing the nidus.
- Selection of the nidus itself (the “region of interest” (ROI)), according to the outline of the target zone for the radiosurgical procedure, as chosen by consensus of six experts (including neurosurgeons, neuroradiologist, radiation oncologist, and physicist).
- Normalization of the intensity of the pixels within the ROI, according to the Brightness Progressive Normalization (BPN) algorithm, introduced by C. Russo [26], which allows to use a single gray-scale threshold for the automatic segmentation of the nidal vessels [10].
- Segmentation of the nidal vessels.
- Application of the box-counting method. A fractal window in a two-order scale was chosen, starting at the highest resolution of the MR images ($\epsilon_{\min} = 0.86 \text{ mm}$ – $\epsilon_{\max} = 86 \text{ mm}$). Monofractal behavior was found in such range.

The obtained FD values were statistically compared to (a) several angioarchitectural parameters, commonly used by the neuroradiologist for the qualitative description of the nidus (e.g., arterial enlargement, flow-related or intranidal aneurysms, flow pattern, neoangiogenesis, venous ectasia, nidus size, number of draining veins,

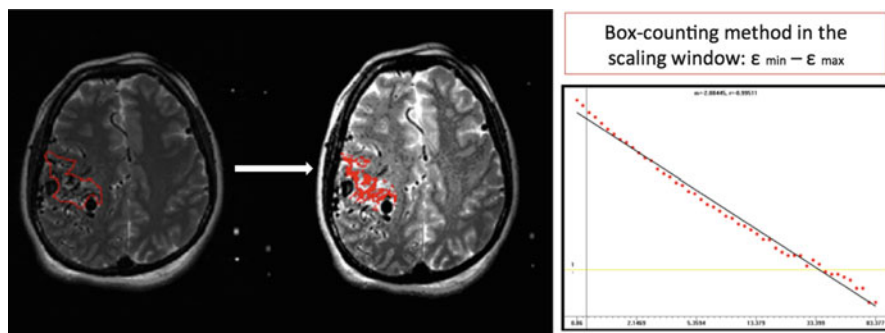


Fig. 18.6 Computation of FD on MR images of AVMs. The region of interest of the AVM is manually segmented on each slice, and an RGB threshold is used for the computer-aided segmentation of the vessels forming the nidus. The box-counting method is then applied in the fractal window, and the results are plotted on a graph, the slope of which represents FD (From Di Ieva et al. [8], reprinted with Permission of the Publisher)

Table

18.1 Angioarchitectural parameters associated with fractal dimension in brain AVMs

Angioarchitectural parameter
Arterial enlargement presence
Presence of non-sprouting angiogenesis
Presence of sprouting angiogenesis
Flow pattern
Venous ectasia
Presence of venous rerouting
Presence of pseudo-phlebitic pattern
Size

venous drainage type, presence of pseudo-phlebitic pattern, etc.) and (b) the radio-surgical outcome, in terms of obliteration, 3 years after the treatment.

In regard to the angioarchitectural parameters, FD was strongly associated with volume and size of the nidus, and significant associations were also found with several other indices (Table 18.1). These results suggested that FD is able to quantify in a single and objective value what neuroradiologists otherwise describe in qualitative and/or semiquantitative way, confirming FD as a reliable morphometric neuroimaging biomarker of AVMs. Higher FD values may signify that the AVM has more tortuous and compact vessels within the nidus, for example, with a higher grade of roughness.

Regarding the outcome, only few morphometric parameters were significantly associated with it, including the presence of sprouting angiogenesis, moderate-to-high flow pattern, and the presence of a venous pouch. Size and venous drainage were both strongly related to outcome, signifying that bigger AVMs (>3 cm of diameter) and/or with deep venous drainage are more related to incomplete obliteration, with a lower chance to be completely cured by means of GK radiosurgery alone. Although no statistical significance was found, interestingly enough the

AVMs with higher FD values had a lower chance of complete obliteration at the follow-up (i.e., lower response to GK) (Fig. 18.7). Every increase in FD value by 0.1 was associated to a 1.21 increase of odds to get an incomplete obliteration. This inverse relationship between FD and AVM obliteration should be further investigated, but at least it would suggest that the fractal analysis may add some parameters to the morphometric of AVMs to predict whether a patient will respond or not to radiosurgery alone and whether he/she will require alternative treatment or a combination of therapeutic modalities (e.g., embolization and/or surgery for “pruning” the nidus, followed by radiosurgery to obliterate the remaining fistulous vessels). The potential of FD as clinical surrogate biomarker for prognosis should be further investigated in larger prospective studies.

Moreover the technique could be extended to other neuroimaging modalities (e.g., DSAs), as well as to the same sequence imaged over time, in order to make a longitudinal analysis of FD during the patients’ follow-up. The longitudinal analysis could offer some indices for prognostication too. For example, in a case in which an AVM is radiologically followed over time (e.g., every 6 months), if the FD values remain constant, it may signify that the patient most likely is a nonresponder to

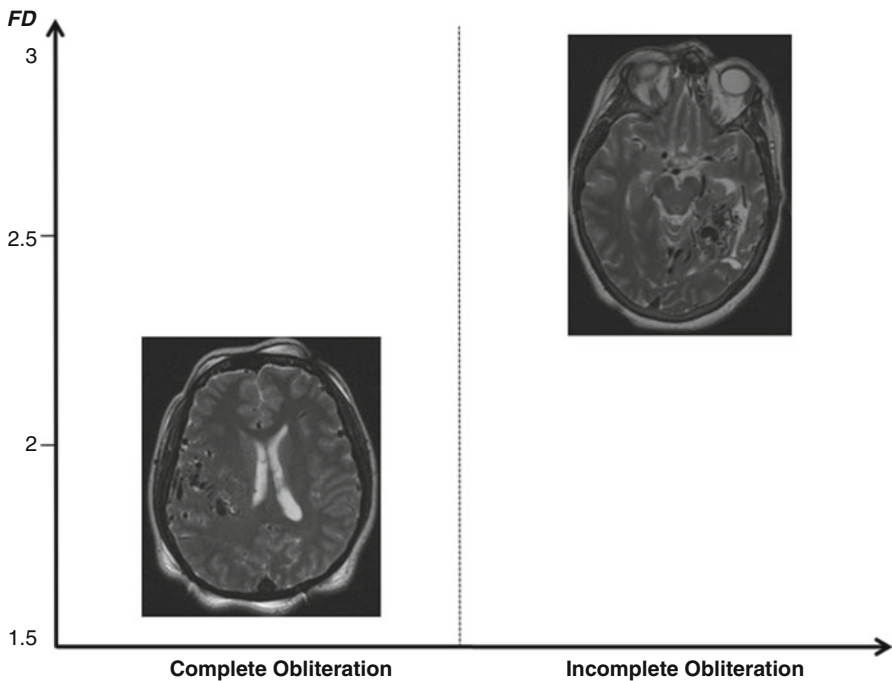


Fig. 18.7 Relating between AVMs’ angioarchitecture (quantified by means of FD) and radiosurgical outcome: the nidus with lower geometrical complexity (lower computed fractal dimension, on the *left*) might have higher chance to be completely obliterated after Gamma Knife radiosurgery treatment, while an incomplete obliteration could occur in a more geometrical complex nidus (higher FD, on the *right*) (From Di Ieva et al. [8], reprinted with Permission of the Publisher)

radiosurgery and may require further treatment (e.g., multimodal treatment with endovascular embolization and/or microneurosurgery). More studies are warranted to validate such computational methods for the assessment of the AVM angioarchitecture in relation to the outcome.

18.5 Limitations

As it may occur in several other neuroimaging analyses, the major limitation of the application of fractal analysis to AVMs' morphometrics is related to the image analysis itself, i.e., to the choice of the ROI (the edges of the nidus). This procedure is in fact generally performed on a consensus of experts, who may introduce some intra- and interobserver variability; moreover, it is time-consuming too. The imaging parameters, as well as the fractal analysis ones, have to be standardized in order to obtain a homogeneous dataset to be analyzed and a homogeneous series of output data, which can correctly be related to some clinical information.

Several techniques are under investigation for the automatic extraction of the ROI as well as for the standardization of the methods of segmentation of the intracranial vessels, as summarized in the following paragraph.

18.6 Computational Techniques for the Automatic Nidus Identification

Several computational techniques are under investigation for the automatic extraction of the nidus' edge from the neuroradiological images. The pixel profiling technique is one of the most promising methods to classify and automatically extract the nidus' edges, by means of a computerized analysis of the pixel intensity distribution inhomogeneity [5]. Threshold-based segmentation of the AVM's vascular tree or voxel-wise support vector machine (SVM) and fuzzy logic have been proposed also as a novel and promising means for fast image extraction of the nidus and therapy planning [4, 14, 15].

Computational fractal-based methods have been investigated as well for the computer-aided identification of the nidus [8]. Lahmiri et al. recently computed FD of cerebral hemispheres via the scaling exponent of detrended fluctuation analysis (DFA), using it in an SVM to differentiate the nonpathologic cerebral hemisphere from the one affected by an AVM, obtaining a perfect classification accuracy [18] (see also Chap. 19). A further method for the automatic detection of AVMs in MR images was developed by computing several fractal-based parameters (including the Hurst exponent) into a supervised machine-learning algorithm, resulting in a computational method for the ROI detection as well as a further conformation of the fractal properties and scale-invariant structure of the AVMs (see methods in [18]). Moreover, assuming that the different pixel distribution within the nidus in MR

imaging may affect the variance (or clustering volatility) of the general pixel distribution in images of normal brains, the generalized autoregressive conditional heteroskedasticity (GARCH) technique, initially proposed for clustering financial time series data [6], was applied for quantifying such differences [8]. The GARCH technique was demonstrated to be potentially helpful in automatically detecting or characterizing the AVMs' nidus.

These computational methods seem to be promising for the automatic segmentation and features extraction of the AVMs, but should be tested on different images (different MRI sequences as well other modalities, including CTAs and DSAs) and on larger patients' series.

18.7 Conclusion

Fractal analysis is a novel approach to quantify the vascular complexity of the arteriovenous malformations. Higher FD values are related to AVMs characterized by an increased number and tortuosity of the intranidal vessels, or to an increasing angioarchitectural complexity as a whole, confirming FD as a reliable computational morphometric neuroimaging biomarker. Moreover FD might be a potential surrogate biomarker for treatment response as well, relevant for prognostication. Fractal analysis can add some parameters, which could be added into a multiparametric morphometric analysis of the angioarchitecture of the nidus itself in relation to some relevant clinical information. The use of lacunarity should be also investigated as angiostructural morphometric parameter. Further studies are required to extend the application of fractal analysis for the study of AVMs.

References

1. Al-Shahi R, Warlow C. A systematic review of the frequency and prognosis of arteriovenous malformations of the brain in adults. *Brain*. 2001;124:1900–26.
2. Andrade-Souza YM, Zadeh G, Ramani M, Scora D, Tsao MN, Schwartz ML. Testing the radiosurgery-based arteriovenous malformation score and the modified spetzler-martin grading system to predict radiosurgical outcome. *J Neurosurg*. 2005;103:642–8.
3. Aoki Y, Nakagawa K, Tago M, Terahara A, Kurita H, Sasaki Y. Clinical evaluation of gamma knife radiosurgery for intracranial arteriovenous malformation. *Radiat Med*. 1996;14:265–8.
4. Babin D, Spyranis M, Pizurica A, Philips W. Pixel profiling for extraction of arteriovenous malformation in 3-D CTA images. *Conf Proc IEEE Eng Med Biol Soc*. 2013;2013:5449–52.
5. Babin D, Pizurica A, Bellens R, De Bock J, Shang Y, Goossens B, et al. Generalized pixel profiling and comparative segmentation with application to arteriovenous malformation segmentation. *Med Image Anal*. 2012;16:991–1002.
6. Bollerslev T. Generalized autoregressive conditional heteroskedasticity. *J Econ*. 1986;31:307–27.
7. Di Ieva A, Esteban FJ, Grizzi F, Klonowski W, Martin-Landrove M. Fractals in the neurosciences, part II: clinical applications and future perspectives. *Neuroscientist*. 2015;21:30–43.
8. Di Ieva A, Boukadoum M, Lahmiri S, Cusimano MD. Computational analyses of arteriovenous malformations in neuroimaging. *J Neuroimaging*. 2014;25:354–60.

9. Di Ieva A, Niamah M, Menezes RJ, Tsao M, Krings T, Cho YB, et al. Computational fractal-based analysis of brain arteriovenous malformation angioarchitecture. *Neurosurgery*. 2014;75:72–9.
10. Di Ieva A, Matula C, Grizzi F, Grabner G, Trattnig S, Tschabitscher M. Fractal analysis of the susceptibility weighted imaging patterns in malignant brain tumors during antiangiogenic treatment: technical report on four cases serially imaged by 7 T magnetic resonance during a period of four weeks. *World Neurosurg*. 2012;77:785.e11–e21.
11. Du R, Keyoung HM, Dowd CF, Young WL, Lawton MT. The effects of diffuseness and deep perforating artery supply on outcomes after microsurgical resection of brain arteriovenous malformations. *Neurosurgery*. 2007;60:638,46; discussion 646–8.
12. Falconer K. *Fractal geometry: mathematical foundations and applications*. New Jersey: Wiley; 2003.
13. Flickinger JC, Pollock BE, Kondziolka D, Lunsford LD. A dose-response analysis of arteriovenous malformation obliteration after radiosurgery. *Int J Radiat Oncol Biol Phys*. 1996;36:873–9.
14. Forkert ND, Illies T, Goebell E, Fiehler J, Saring D, Handels H. Computer-aided nidus segmentation and angiographic characterization of arteriovenous malformations. *Int J Comput Assist Radiol Surg*. 2013;8:775–86.
15. Forkert ND, Schmidt-Richberg A, Fiehler J, Illies T, Moller D, Saring D, et al. 3D cerebrovascular segmentation combining fuzzy vessel enhancement and level-sets with anisotropic energy weights. *Magn Reson Imaging*. 2013;31:262–71.
16. Jenkinson M, Smith S. A global optimisation method for robust affine registration of brain images. *Med Image Anal*. 2001;5:143–56.
17. Kanmani S, Rao CB, Raj B. On the computation of the minkowski dimension using morphological operations. *J Microsc*. 1993;170:81–5.
18. Lahmiri S, Boukadoum M, Di Ieva A. Detrended fluctuation analysis of brain hemisphere magnetic resonance imaging to detect cerebral arteriovenous malformations. *Circuits and Systems (ISCAS), IEEE International Symposium*. 2014;2409–12.
19. Lopes R, Betrouni N. Fractal and multifractal analysis: a review. *Med Image Anal*. 2009;13:634–49.
20. Matsumoto M, Kodama N, Endo Y, Sakuma J, Suzuki K, Sasaki T, et al. Dynamic 3D-CT angiography. *AJNR Am J Neuroradiol*. 2007;28:299–304.
21. McGee KP, Ivanovic V, Felmlee JP, Meyer FB, Pollock BE, Huston 3rd J. MR angiography fusion technique for treatment planning of intracranial arteriovenous malformations. *J Magn Reson Imaging*. 2006;23:361–9.
22. Ondra SL, Troupp H, George ED, Schwab K. The natural history of symptomatic arteriovenous malformations of the brain: a 24-year follow-up assessment. *J Neurosurg*. 1990;73:387–91.
23. Pollock BE, Lunsford LD, Kondziolka D, Maitz A, Flickinger JC. Patient outcomes after stereotactic radiosurgery for “operable” arteriovenous malformations. *Neurosurgery*. 1994;35:1,7; discussion 7–8.
24. Pruess SA. Some remarks on the numerical estimation of fractal dimension. In: Barton CC, La Pointe PR, editors. *Fractals in the earth sciences*. New York: Plenum Press; 1995. p. 10.
25. Reishofer G, Koschutnig K, Enzinger C, Ebner F, Ahammer H. Fractal dimension and vessel complexity in patients with cerebral arteriovenous malformations. *PLoS One*. 2012;7:e41148.
26. Russo C. Brightness progressive normalization. 2012. Webpage: http://www.fractal-lab.org/Downloads/bpn_algorithm.html. Accessed on Feb 2016.
27. Spetzler RF, Ponce FA. A 3-tier classification of cerebral arteriovenous malformations. *Clinical article*. *J Neurosurg*. 2011;114:842–9.
28. Spetzler RF, Martin NA. A proposed grading system for arteriovenous malformations. *J Neurosurg*. 1986;65:476–83.
29. Wu Y, Chang W, Johnson KM, Velikina J, Rowley H, Mistretta C, et al. Fast whole-brain 4D contrast-enhanced MR angiography with velocity encoding using undersampled radial acquisition and highly constrained projection reconstruction: image-quality assessment in volunteer subjects. *AJNR Am J Neuroradiol*. 2011;32:E47–50.